# Investigation of the Protonation State of Novel Cationic Lipids Designed for Gene Transfection

**Maria N. Antipina,*,† Bodo Dobner,‡ Oleg V. Konovalov,§ Vladimir L. Shapovalov,|| and Gerald Brezesinski*,†**

*Max Planck Institute of Colloids and Interfaces, Research Campus Golm, Am Muehlenberg 1, D-14476 Potsdam, Germany, Institute of Pharmacy, Martin-Luther-University, Wolfgang-Langenbeck-Str. 4, D-06120 Halle/S., Germany, European Synchrotron Radiation Facility, BP-220, E-38043, Grenoble, France, and N. N. Semenov Institute of Chemical Physics RAS, ul. Kosygina 4, 119991 Moscow, Russia*

*Received: July 16, 2007; In Final Form: August 23, 2007*

In order to be used in versatile DNA delivery systems, novel cationic lipids were synthesized. The head groups of the new compounds represented by monoamines or oligoamines can be charged or uncharged depending on the environmental pH. Since their p*K* values are unknown, the protonation properties of these lipids have been studied in a wide pH range. In our experiments, the amphiphilic molecules were organized as a Langmuir monolayer at the air−water interface. Total reflection X-ray fluorescence (TRXF) was used to determine the 2D concentration of bromide counterions bound to a positively charged (protonated) Langmuir monolayer. The protonation rate of the novel cationic lipids was estimated by comparing the fluorescence intensity with that of dioctadecyldimethylammonium bromide monolayers as a reference. TRXF investigations were supplemented with results of film-balance measurements, grazing incidence X-ray diffraction, and X-ray reflectivity data. The results obtained display that the monolayers of all studied compounds are completely uncharged at pH values above 10. In the investigated pH region, the highest protonation rate of the monolayers is observed at pH 3. The influence of the monolayer packing density on the protonation properties is clearly shown.

## Introduction

One of the most important purposes of contemporary molecular biology and human clinical gene therapy is the transfection of extracellular genetic material into eukaryotic cells. Complexes consisting of DNA mixed with oppositely charged cationic liposomes mimic natural viruses in their ability to carry DNA-based therapeutics across cell and nuclear membranes. In spite of the fact that liposomal delivery systems are safer drugs in comparison with viral vectors, they often fail in practical use of gene therapy because of low effectiveness. Therefore, fabrication of liposomes that contain target and functionalized groups in their lipid bilayers and are tailor-made for a range of specialized DNA delivery options appeared to be a promising strategy.[1] For example, liposomes containing an antibody fragment against the human transferrin receptor were successfully used in targeted delivery of tumor-suppressing genes into tumors in vivo.[2] Tissue-specific gene delivery using liposomes has been achieved in the brain, embryonic tissue, and breast cancer tissue.[3−5] Another important property of liposomal formulations which can enhance their effectiveness is pH-sensitivity providing protection of DNA drugs in acidic environment of the endosome and in situ release of genetic material.[6−7] The other problem of artificial vector delivery systems is cytotoxicity of lipids used for liposomes formation. Toxicity of lipids if not completely eliminated must be however as low as possible. For that purpose, new cationic lipids (Figure 1) were synthesized. Further introduction of specific ligands for selective targeting to cells and tissues will let the new compounds serve as multifunctional delivery platforms. The chemical structure of the new lipids makes them promising candidates for pH-sensitive liposomes. In a previous study, it was shown that the monolayer structure and the physical-chemical properties of 2-amino-3-hexadecyloxy-2-hexadecyloxymethyl-propan-1-ol are strongly influenced by the subphase pH.[8] However, the p*K* values of the novel cationic compounds are still unknown but of particular importance for further practical applications. In this work, the protonation state of the novel cationic compounds organized as Langmuir monolayers on aqueous subphases was investigated in a wide range of pH. Total reflection X-ray fluorescence (TRXF) technique has been utilized as a tool to obtain quantitative information about the concentration of counterions adsorbed to charged lipid molecules.[9,10] The TRXF study was supplemented and coupled with film balance measurements and X-ray scattering experiments.

## Experimental Section

For all measurements and sample preparations, Milli-Q Millipore water with a specific resistance of 18.2 MΩ·cm was used. The novel cationic lipids 2-tetradecylhexadecanoic acid-{2-[(2-aminoethyl)amino]ethyl}amide (CI), 2-tetradecylhexadecanoic acid-2-[bis(2-aminoethyl)amino]ethylamide (CII), *N*-{2-[bis(2-aminoethyl)amino]ethyl}-2,*N*′-dihexadecyl-propandiamide (CIII), and 2-amino-3-hexadecyloxy-2-hexadecyloxymethyl-propan-1-ol (CIV) (Figure 1) were synthesized in the

* To whom correspondence should be addressed. Tel: +49 331 567 9232. Fax: +49 331 567 9202. E-mail: maria.antipina@mpikg.mpg.de (Maria N. Antipina). Tel: +49 331 567 9234. Fax: +49 331 567 9202. E-mail: brezesinski@mpikg.mpg.de (Gerald Brezesinski).

† Max Planck Institute of Colloids and Interfaces.

‡ Martin-Luther-University.

§ European Synchrotron Radiation Facility.

|| N. N. Semenov Institute of Chemical Physics RAS.

10.1021/jp0755591 CCC: $37.00 
Published on Web 11/17/2007

2-tetradecylhexadecanoic acid-{2-[(2-aminoethyl)amino]ethyl}amide (CI)

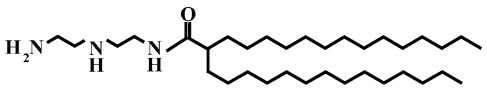

2-tetradecylhexadecanoic acid-2-[bis(2-aminoethyl)amino]ethylamide (CII)

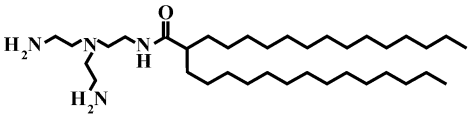

N-{2-[bis(2-aminoethyl)amino]ethyl}-2,N′-dihexadecyl-propandiamide (CIII)

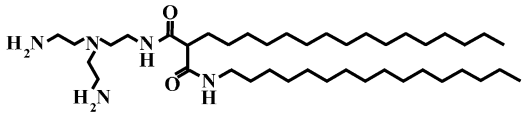

2-amino-3-hexadecyloxy-2-hexadecyloxymethyl-propan-1-ol (CIV)

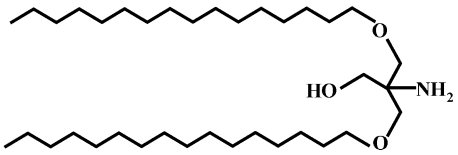

**Figure 1.** Chemical structures of newly synthesized cationic lipids.

Institute of Pharmacy, Martin-Luther-University, Halle, Germany. The synthesis of CIV has been already described,[8] and the synthesis of the other compounds will be described in a separate manuscript. The compounds were characterized by ESI-MS, elemental analysis and $^1$H NMR.

CI: $C_{34}H_{71}N_3O$, 537,93 g·mol$^{-1}$, fp 96−99 °C. ESI-MS *m*/*e* 539 ($M^+ + H$), calcd C 75.91, H 13.30, N 7.81: found C 76.35, H 13.20, N 7.11. $^1$H NMR ($CDCl_3$): $\delta = 0.84$ (m, 6H, 2[C**H**$_3$-$(CH_2)_{13}$-]), 1.2−1.5 (m, 54H, 2[$CH_3$(C**H**$_2$)$_{13}$, [**H**$_2$N-]), 2.62−2.67 (m, 4H, [$H_2$NC**H**$_2$$CH_2$NH-],[-HNC**H**$_2$$CH_2$NH-]), 2.78−2.88 (m, 2H, [$H_2$N$CH_2$C**H**$_2$NH-]), 3.0−3.08 (m,1H, [-C**H**-]), 3.38−3.40 (m, 2H, [-NH$CH_2$C**H**$_2$NHCO-]), 4.1−4.2 (m, 2H, 2[-N**H**-]), 6.50−6.55 (m, 1H, [-N**H**CO-]).

CII: $C_{36}H_{76}N_4O$, 581.02 g·mol$^{-1}$, fp 73−75 °C. ESI-MS *m*/*e* 582 ($M^+ + H$), calcd C 74.42, H 13.18, N 9.64; found C 74.32, H 13.11, N 9.70. $^1$H NMR ($CDCl_3$): $\delta = 0.85$ (t, 6H, 2[C**H**$_3$-$(CH_2)_{15}$-]), 1.21−1.57 (m, 64H, 2[$CH_3$(C**H**$_2$)$_{15}$-], 2[**H**$_2$N-]), 2.00−2.14 (m, 4H, 2[$H_2$N$CH_2$C**H**$_2$-]), 2.53−2.58 (m, 4H, 2[$H_2$-NC**H**$_2$$CH_2$-]), 2.78 (t, 2H, [-NC**H**$_2$$CH_2$NH-]), 3.13−3.20 (m, 1H, [-C**H**-], 3.29−3.34 (m, 2H, [-N$CH_2$C**H**$_2$NH-]), 7.06 (s, 1H, [-CON**H**-]).

CIII: $C_{41}H_{85}N_5O_2$, 680.15 g·mol$^{-1}$, fp 84−86 °C, ESI-MS *m*/*e* 681 ($M^+ + H$), calcd C 72.40, H 12.60, N 10.30; found C 72.27, H 12.48, N 10.25. $^1$H NMR ($CDCl_3$/$CD_3OD$): $\delta = 0.86$ (t, 6H, 2[C**H**$_3$$(CH_2)_{15}$-]), 1.22−1.79 (m, 58H, [$CH_3$(C**H**$_2$)$_{15}$-], [$CH_3$(C**H**$_2$)$_{14}$$CH_2$NH]), 2.03 (s, 4H, 2[N**H**2-]), 2.51−2.56 (m, 4H, 2[-$NH_2CH_2$C**H**$_2$-]), 2.73−2.76 (m, 4H, 2[$NH_2$C**H**$_2$$CH_2$-]), 2.96 (t, 2H, [-NC**H**$_2$$CH_2$NH-]), 3.13−3.20 (m, 2H, [$CH_3$-$(CH_2)_{14}$C**H**$_2$NH-]), 3.21−3.35 (m, 2H, [-N$CH_2$C**H**$_2$NH-]), 3.60−3.63 (m,1H, [$CH_3(CH_2)_{15}$C**H**-]), 6.89 (t, 1H [-CON**H**$(CH_2)_{15}$-]), 8.34 (t, 1H, [CON**H**$(CH_2)_2$-]).

Dioctadecyldimethylammonium bromide (DODAB) used as the reference substance for the evaluation of TRXF measurements was purchased from Fluka. All chemicals used for the preparation of buffer subphases were obtained from Sigma Aldrich. In the pH range from 4 up to 10, 2-morpholinoethylamine (p$K_{a1}$ = 4.8, p$K_{a2}$ = 9.5), piperazine (p$K_{a1}$ = 5.7, p$K_{a2}$ = 9.8), BIS-TRIS propane (p$K_{a1}$ = 6.8, p$K_{a2}$ = 9.0), or 1,4-diazabicyclo(2,2,2)octane (p$K_{a1}$ = 4.2, p$K_{a2}$ = 8.2) were used as basic species. According to the purpose of TRXF measurements, HBr in a constant concentration of 2 mM was chosen as the acid species. The subphase with pH 11 was obtained using 2 mM of NaBr and KOH.

For monolayer experiments, 1 mM stock solutions of each cationic lipid were prepared in chloroform (Merck, Germany; purity >99.8%). The corresponding solution was placed on the aqueous subphase by a microsyringe and allowed to relax for 5 min before compression for the evaporation of the solvent. The pressure/area ($\pi$-A) isotherms were recorded during compression of the monolayer on the computer-interfaced Langmuir trough (R&K, Potsdam, Germany). The compression rate of the films was approximately 2 Å$^2$·molecule$^{-1}$·min$^{-1}$. The setup is equipped with a Wilhelmy balance to measure the monolayer surface pressure $\pi$ and has a temperature control system. The subphase temperature was maintained at 20 °C with an accuracy of ±0.1 °C.

TRXF measurements were carried out at the high-brilliance undulator beamline Troika II (ID10B) of the European Synchrotron Radiation Facility (ESRF), Grenoble, France. The experimental setup includes a Langmuir trough specially designed for the X-ray experiments. The Langmuir monolayer was compressed to a desired surface pressure, which was kept constant during the measurements. All measurements were done in air at room temperature.

The synchrotron X-ray beam coming from the undulator is first reflected from the diamond (111) monochromator crystal in symmetric Bragg geometry which acts as a beam splitter deflecting a narrow energy band of radiation in horizontal geometry. Both incoming and reflected beams lie in the horizontal plane. The second crystal, working in the regime of symmetric reflection, deflected the monochromatic beam back to the initial direction. A compact double-mirror setup is used for a strong suppression of higher harmonics. In the standard geometry, the first mirror deflects the beam up and the second mirror reflects the beam back horizontally. Both mirrors are placed in an ultrahigh vacuum chamber. The monochromatic and cleaned from the higher harmonics beam was deflected from the horizontal plane and sent to the liquid surface at a fixed angle of incidence of 0.035° (which corresponds to 60% of the critical angle of total reflection for water at 22 keV photon energy) with respect to the horizontal liquid surface by means of rotation of the deflecting crystal (Ge) around the incident beam with keeping the Bragg reflection condition for Ge (111) reflection. The reflected beam was detected by a scintillation (NaI) detector. The fluorescent signal was measured by a Peltier cooled ROENTEC drift diode Si detector oriented normal to the liquid surface. The axis of the incident beam and the view directions of the NaI and ROENTEC detectors were lined up so that they crossed at the same point. The surface of the liquid was adjusted to this point before each measurement of the fluorescence signal.

Grazing incidence X-ray diffraction (GIXD) and X-ray reflectivity (XR) measurements were performed using the liquid surface diffractometer (undulator beamline BW1) at HASYLAB,

DESY, Hamburg, Germany.[11,12] The Langmuir trough is located in a thermostated, tightly closed and He-filled container. A monochromatic beam ($\lambda = 1.304$ Å) from a beryllium (002) crystal strikes the water surface at an angle of 0.11° equal to 85% of the critical angle of total external reflection of water for this X-ray wavelength. A linear position sensitive detector (PSD) (OED-100-M, Braun, Garching, Germany) with a vertical acceptance $0 < Q_z < 1.27$ Å$^{-1}$ was used for recording the diffracted intensity as a function of both the vertical ($Q_z \approx (2\pi/\lambda)\sin(\alpha_f)$) (where $\alpha_f$ is the vertical scattering angle) and the horizontal ($Q_{xy} \approx (4\pi/\lambda)\sin(2\Theta_{hor}/2)$) scattering vector components. The tilt angle t is the angle between the normal to the water surface and the symmetry axis of the hydrocarbon chain. In the case of an orthorhombic lattice with chains tilted toward the nearest neighbors (NN), the tilt angle can be calculated by.[13,14]

$$\tan(t) = \frac{Q_z^{\mathrm{d}}}{\sqrt{(Q_{xy}^{\mathrm{d}})^2 - (Q_{xy}^{\mathrm{n}}/2)^2}} \quad (1)$$

where d and n indicate the degenerate and nondegenerate Bragg peaks, respectively.

Using a NaI scintillation detector, the X-ray reflectivity was measured as a function of the vertical incidence angle, $\alpha_i$, with the geometry $\alpha_i = \alpha_f = \alpha$, where $\alpha_f$ is the vertical exit angle of the reflected X-rays. The background scattering from, e.g., the subphase was measured at $2\theta_{hor} = 0.7°$ and subtracted from the signal measured at $2\theta_{hor} = 0°$. XR data were analyzed by model-independent inversions of the experimental results using b-splines $B_i(z)$ to describe the electron density distribution normal to the surface

$$\rho(z) = \sum_{i=1}^{N} \alpha_i B_i(z) \quad (2)$$

where $N$ is determined by the accessible $Q_z$ range via the sampling theorem.[15,16] The electron density $\rho(z)$, which is laterally averaged over both the ordered and disordered parts in the footprint of the beam, can be modeled by a stack of homogeneous "boxes" with variable thickness, electron density, and roughness.[17,18]

## Results and Discussion

The cationic groups of the newly synthesized lipids are represented either by oligoamines (CI, CII, and CIII) or by monoamine (CIV), which can be protonated and therefore positively charged or deprotonated/uncharged depending on the environmental pH value. The pH-dependent protonation of the head group markedly alters the pressure/area ($\pi-A$) isotherms of the monolayers as shown in Figure 2. Electrostatic repulsion between charged head groups leads to an expansion of the monolayer (shift to larger molecular areas) at pH 3 in comparison with pH 11 (or with pH 10 in the case of CIV) which presumably corresponds to the uncharged state of the molecules at the interface. In the case of CIII, the decrease of pH promotes the fluidization of the monolayer at low surface pressure values. The pressure of the transition from the liquid-expanded to the liquid-condensed state increases with decreasing pH. The large molecular area observed for the monolayers of CI and CII indicates that these monolayers are fluid at all investigated pH values. In contrast, the monolayer of CIV is fully condensed on all buffer subphases. Thus, electrostatic repulsion due to protonation of the head group is obviously not strong enough to compete successfully with the strong van der Waals attraction between neighboring chains.

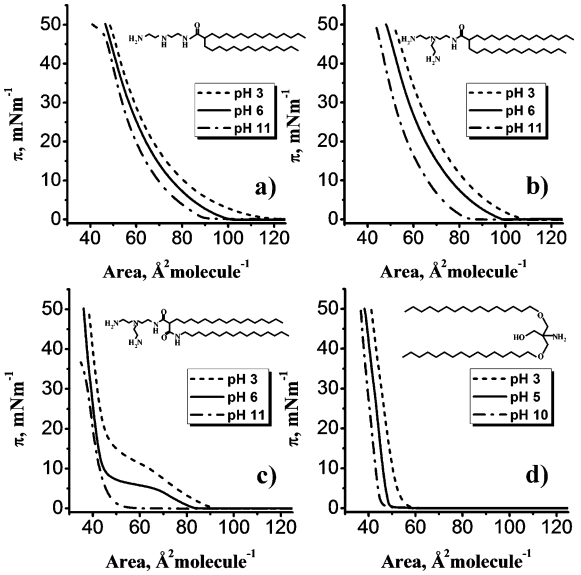


**Figure 2.** Pressure/area isotherms of the monolayers of CI (a), CII (b), CIII (c), and CIV (d) on subphases with different pH (indicated) at 20 °C.

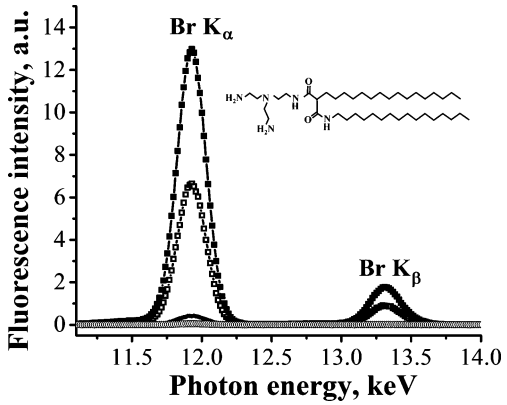


**Figure 3.** Selected X-ray fluorescence spectra of the CIII Langmuir monolayer at 40 Å$^2$·molecule$^{-1}$ on $Br^-$ containing subphases at pH 3 (■), pH 6 (□), pH 8 (●), and pH 11 (○).

Compression isotherms of the investigated lipids recorded on subphases with pH 4 and 5 (data not shown) were nearly overlapping with those on the pH 3 buffer subphase. The same tendency to overlap was observed for compression isotherms of lipid monolayers on subphases with pH between 7 (or 6, as in the case of CIV) and 11. Obviously, the observed small variations of the protonation rate (see Figure 4) in the corresponding pH regions have no clear influence on the isotherms. This shows that using only isotherm measurements is not sufficient to estimate the protonation rate of such molecules.

The background of the TRXF method and its application for the investigation of counterion concentrations at interfaces were described in detail elsewhere.[10] TRXF was used in order to quantify the effect of pH on the protonation state of the new molecules. The monolayers of CI− CIV were formed on subphases with a constant concentration (2 mM) of $Br^-$ anions, and the X-ray fluorescence intensity of Br, which is proportional to the amount of $Br^-$ anions coupled to the protonated lipid head groups, was measured in dependence on the bulk-phase pH. Selected X-ray fluorescence spectra of CIII are presented in Figure 3. The Br K$\alpha$ and Br K$\beta$ fluorescence peaks are well observable. It could be clearly seen that their intensity decreases

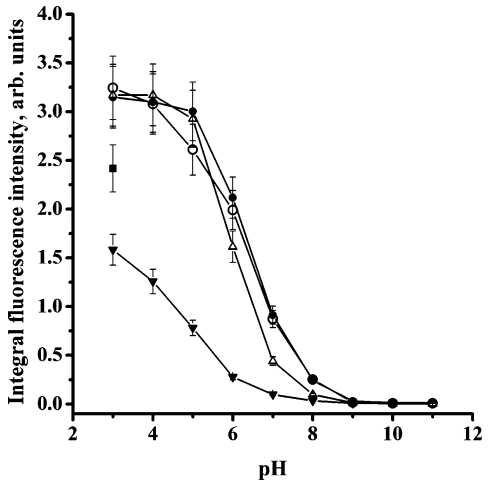


**Figure 4.** Integral X-ray fluorescence intensity from Br− coupled to the Langmuir monolayers of DODAB at 50 Å$^2$·molecule$^{-1}$ (■), CI at 64 Å$^2$·molecule$^{-1}$ (○), CII at 60 Å$^2$·molecule$^{-1}$ (●), CIII at 40 Å$^2$·molecule$^{-1}$ (△), and CIV at 43 Å$^2$·molecule$^{-1}$ (▼) in dependence on the subphase pH.

with increasing pH and is close to 0 at pH 11. The same tendency was observed for all other compounds. As the fluorescence intensity depends on the 2D concentration of bromide anions at the charged surface, it was important to measure the X-ray spectra at approximately the same molecular area for each compound for further comparison. The fluid CI and CII monolayers have been measured at 64 and 60 Å$^2$·molecule$^{-1}$, respectively. Spectra of the condensed monolayers of CIII and CIV were taken at 40 and 43 Å$^2$·molecule$^{-1}$, respectively.

Plotting the integral intensity of fluorescence peaks versus pH one can obtain a titration curve for each investigated lipid (Figure 4). Except for compound IV, the slope of these curves levels off within the limits of the error bars below pH 4. Above pH 9 in the case of CIV or pH 10 in the case of the other cationic lipids, the intensity drops to zero indicating that the head groups are fully deprotonated.

In order to get quantitative information about the protonation rate and/or the number of protonated groups in the head group region of the cationic lipids CI−CIV, the X-ray fluorescence spectrum of a DODAB monolayer on a $Br^-$ containing aqueous subphase was measured as a reference. The quaternary ammonium head group ensures one permanent positive charge of DODAB independent of pH conditions. Therefore, the integral fluorescence intensity from the DODAB monolayer has been taken as a reference to evaluate the surface charge density of CI, CII, CIII, and CIV.

In order to compare the fluorescence intensity from $Br^-$ anions coupled to Langmuir monolayers of different substances, one should take into account that the experimentally observed intensity of the fluorescence signal $I$ is directly proportional to the protonation rate of the monolayer molecules $p$, the surface concentration of amphiphiles $C_{surface}$, and the intensity of the evanescent wave ($I_e$)

$$I \sim pC_{surface}I_e \tag{3}$$

The amplitude of the evanescent wave decays exponentially from the monolayer interface as described by the relationship[19]

$$I_e = I_0 \exp\left(-\frac{z}{\Lambda}\right) \tag{4}$$

**TABLE 1: Positions of Bragg Peak ($Q_{xy}$) and Bragg Rod ($Q_z$) Maxima and Calculated Tilt Angle $t$ of the Hydrocarbon Chains of Cationic Lipid Monolayers in the Condensed State (pH 3)**

| substance | $\pi$, mNm$^{-1}$ | $Q_{xy}1$, Å$^{-1}$ | $Q_z1$, Å$^{-1}$ | $Q_{xy}2$, Å$^{-1}$ | $Q_z2$, Å$^{-1}$ | $t$, ° |
|---|---|---|---|---|---|---|
| DODAB | 40 | 1.408 | 0 | 1.349 | 0.765 | 33.6 |
| CIII | 40 | 1.496 | 0 | - | - | 0 |
| CIV | 39.6 | 1.478 | 0 | 1.452 | 0.42 | 18.6 |

where $I_0$ is the maximum electric field intensity, $z$ is the distance from the interface, and $\Lambda$ is the penetration depth (decay length) for the evanescent wave in the aqueous subphase. Therefore, the monolayer protonation rate appeared to be directly proportional to $k$

$$p \sim k = \frac{I}{C_{surface}\exp\left(-\frac{z}{\Lambda}\right)} \tag{5}$$

For hard X-rays, it was shown that the penetration depth is close to 5 nm at incident angles $\alpha_i$ well below the critical angle $\alpha_c$.[11,20]

In the case of Langmuir monolayers at the air−water interface, $z$ corresponds to the thickness of the hydrophobic chain layer. Different approaches were used to estimate the $z$ values. In condensed monolayers, the alkyl chains are in all-trans conformation. Therefore, $z$ can be directly estimated using the theoretical length of a stretched chain and its tilt angle $t$ to the surface normal. The mean distance between $CH_2$ groups along the chain axes of aliphatic chains in all-trans conformation is 1.26 Å.[21,22] The maximum length[23] of a stretched alkyl chain with $n$ $CH_2$ groups amounts to $l_{max} = (n\cdot 1.26 + 1.5)$ Å, so that

$$z = l_{max}\cos(t) \tag{6}$$

Information about the tilt angle of lipid chains in the condensed phases of DODAB, CIII, and CIV was obtained by grazing incidence X-ray diffraction measurements. GIXD data together with the calculated values of molecular tilt are presented in Table 1.

The thickness of the fluid monolayers was derived from X-ray reflectivity data. XR of CI and CII monolayers at the air−buffer interface has been measured and fitted with a free-form model. The electron density profiles derived from this approach were described by a two-box model. The molecular area determined from the isotherm and the number of electrons in the hydrophobic part of the molecule were used as fixed parameters during the fitting procedure. The hydrocarbon chains layer has a thickness of $z = (12.2 \pm 0.5)$ Å in the case of CI. As the hydrophobic chains of CI and CII are of the same length one can expect similar parameters for the monolayers of these lipids. Indeed the obtained value $z = (12.3 \pm 0.5)$ Å confirms this assumption (Table 2). The $z$ values obtained by sophisticated X-ray scattering methods can also be estimated by the simple consideration that $z$ depends on the molecular weight of the hydrophobic chains ($MW_{hch}$), the monolayer area per molecule ($A$) and the density of the hydrophobic layer ($\rho$)

$$z = \frac{MW_{hch}}{N_a A\rho} \tag{7}$$

with $N_a$ as the Avogadro constant.

The density of polyethylene (0.9 g·cm$^{-3}$) was taken as a good estimate for hydrophobic layers. The thicknesses of the hydrophobic layers calculated for all of the systems using eq 7 are presented in Table 2. It can be seen, that the $z$ values estimated

**TABLE 2: Surface Concentration $C_{surface}$, TRXF Intensity I, Thickness of the Hydrophobic Monolayer Part *z*, and Estimation of the Protonation Rate of Cationic Lipid Langmuir Monolayers on the pH 3 Subphase Using an Average Value of *z***

| substance | $C_{surface}$ (molecule/Å$^2$) | I arb units | *Z* (Å) calculated from GIXD or XR | *Z* (Å) calculated from eq (7) | ($k \pm 10\%$) arb. units |
|---|---|---|---|---|---|
| DODAB | 1/50 | 2.4 | 19.1 | 18.7 | 175 |
| DODAB | 1/101 | 1.5 | | 9.2 | 182 |
| CI | 1/64 | 3.19 | 12.2 | 11.8 | 260 |
| CII | 1/60 | 3.15 | 12.3 | 12.5 | 242 |
| CIII | 1/40 | 3.17 | 20.4 | 21.4 | 193 |
| CIV | 1/43 | 1.56 | 19.3 | 19.3 | 99 |

by different approaches are in a rather good agreement. Therefore, eq 7 can be used as a convenient method to calculate thicknesses of the hydrophobic part of lipid Langmuir monolayers.

The direct comparison of the calculated *k* values (see Table 2) displays that the fluid monolayers of CI and CII have a higher surface charge density than fluid DODAB at approximately the same area per molecule. This indicates that a certain amount of molecules within the monolayer of the novel cationic lipids have more than one protonated amine group. The corresponding *k* values show that ~40% of the CI and CII molecules have two positive charges per head group. Within the limits of the error bars, we can conclude that the CIII molecules carry one positive charge at low pH values.

Our results clearly demonstrate that the protonation properties of monolayers formed by molecules with the same head group structure are different in dependence on the packing density. In fact, *k* is equal to 242 arb. units for CII fluid monolayers at pH 3 and therefore significantly larger compared with 193 arb. units obtained for the condensed monolayer of CIII at the same pH. Thus, the densely packed molecules in the highly ordered condensed monolayer are less protonated in comparison with the fluid layer of molecules with the same head group. This experimental finding seems to be reasonable because the higher surface density of positive charges leads to the decrease of the surface proton concentration according to the Boltzmann equation, what will result in the decrease of the monolayer protonation rate.

The CIV molecules have only one amine group to be protonated. Figure 4 and Table 2 display that less than 100% of the molecules are protonated even at pH 3, as the X-ray fluorescence signal from this monolayer compressed to 43 Å$^2$·molecule$^{-1}$ does not attain the intensity observed with DODAB at an even larger area per molecule. A rough estimation in comparison with DODAB gives a surface charge density of 1 positive charge per 72 Å$^2$ for the CIV monolayer at pH 3. The X-ray observations support the conclusion which can be simply drawn from the chemical structure of the investigated compound. Due to the geometrical arrangement of the four groups attached at the tertiary carbon atom, which are competing for the contact with the aqueous subphase, the protonation of the amine group is hindered. Figure 5 shows the degree of protonation of compound IV as a function of bulk pH calculated from the experimental data shown in Figure 4 (normalized to the DODAB data). Theoretical curves calculated according to an already described procedure[24] based on the Gouy−Chapman model are also shown. The comparison between experimental data and theoretical curves shows that the p$K_a$ value of compound IV is close to 8, which is in very good agreement with the p$K_a$ value of 2-amino-2-(hydroxymethyl)-propane-1,3-diol (TRIS) from which compound IV is derived.

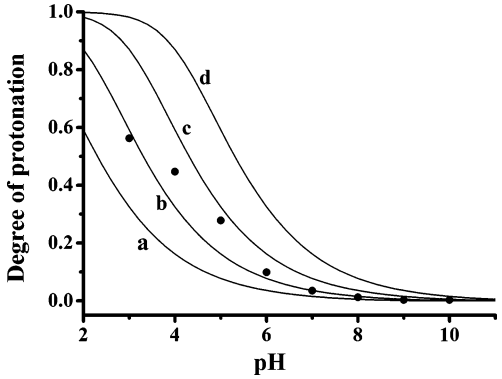


**Figure 5.** Degree of protonation versus bulk pH for compound IV obtained from the TRXF data (●) presented in Figure 4. Theoretical curves ($c = 2$ mM, 43 Å$^2$·molecule$^{-1}$, p$K_a$ of 6 (a), 7 (b), 8 (c), and 9 (d), respectively) based on the Gouy−Chapman model are also presented.

As shown in a previous publication,[8] DNA dissolved in the subphase couples to CIV monolayers at pH 4 as well as at pH 8. Comparing the integrated intensities of the fluorescence peaks of the DODAB and the CIV monolayers on the pH 8 subphase, it becomes evident that only approximately 1% of the CIV molecules in the monolayer can be protonated under that condition. However, even such a low charge density seems to be enough to attract DNA. On the other hand, the coupled DNA should affect the potential of the electrical double layer and therefore change the surface pH in accordance with the Boltzmann equation leading to an increasing protonation rate of the monolayer. This leads to a further binding of DNA molecules.

## Conclusions

Protonation properties of Langmuir monolayers of the newly synthesized cationic lipids 2-tetradecylhexadecanoic acid-{2-[(2-aminoethyl)amino]ethyl}amide, 2-tetradecylhexadecanoic acid-2-[bis(2-aminoethyl)amino]ethylamide, *N*-{2-[bis(2-aminoethyl)amino]ethyl}-2,*N*′-dihexadecyl-propandiamide, 2-amino-3-hexadecyloxy-2-hexadecyloxymethyl-propan-1-ol were investigated in a wide range of subphase pH using film balance measurements, TRXF, GIXD, and XR studies. It was shown that the molecules of all novel compounds are deprotonated at subphase pH values above 9. In contrast, at pH 3 all molecules in the monolayers of CI, CII and CIII carry at least one protonated group. 100% protonation of molecular head groups does not occur in CIV monolayers even at pH 3. It was experimentally confirmed that the protonation rate depends not only on the chemical structure but also on the packing density in the monolayer. In fact, the protonation rate of the fluid monolayer of compound II is 1.4, whereas only 1 positive charge per molecule was found in the case of the condensed monolayer of compound III exhibiting the same head group.

**Acknowledgment.** This work was supported by the Max Planck Society and the Alexander von Humboldt Foundation (M.N.A.). We thank ESRF, Grenoble, France, and HASYLAB, Hamburg, Germany, for beam time and for providing excellent facilities and support. We are grateful to Dr. Christian Symietz (MPI-KGF) for the GIXD results of the DODAB monolayer.

## References and Notes

(1) Fattal, E.; Delattre, J.; Dubernet, C.; Couvreur, P. *S.T.P. Pharm. Sci.* **1999**, *9*, 383.

(2) Xu, L.; Huang, C-C.; Huang, W.; Tang, W-H.; Rait, A.; Yin, Y. Z.; Cruz, I.; Xiang, L-M.; Pirollo, K. F.; Chang, E. H. *Mol. Cancer Ther.* **2002**, *1*, 337.

(3) Shi, N.; Zhang, Y.; Zhu, C.; Boado, R. J.; Pardridge, W. M. *Proc. Natl. Acad. Sci. U.S.A.* **2001**, *98*, 12754.

(4) Khaw, B. A.; da Silva, J.; Vural, I.; Narula, J.; Torchilin, V. P.; *J Controlled Release* **2001**, *75*, 199.

(5) Krauss, W. C.; Park, J. W.; Kirpotin, D. B.; Hong, K.; Benz, C. C. *Breast Dis.* **2000**, *11*, 113.

(6) Venugopalan, P.; Jain, S.; Sankar, S.; Singh, P.; Rawat, A.; Vyas, S. P. *Pharmazie* **2002**, *57*, 659.

(7) Maclean, A. L.; Symonds, G.; Ward, R. *Int. J. Oncol.* **1997**, *11*, 325.

(8) Antipina, M. N.; Schulze, I.; Dobner, B.; Langner, A.; Brezesinski, G. *Langmuir* **2007**, *23*, 3919.

(9) Bloch, J. M.; Sansone, M.; Rondelez, F. *Phys. Rev. Lett.* **1985**, *54*, 1039.

(10) Shapovalov, V. L.; Ryskin, M. E.; Konovalov, O. V.; Hermelink, A.; Brezesinski, G. *J. Phys. Chem. B* **2007**, *111*, 3927.

(11) Als-Nielsen, J.; Jaquemain, D.; Kjaer, K.; Lahav, M.; Levellier, F.; Leiserowitz, L. *Phys. Rep.* **1994**, *246*, 251.

(12) Kaganer, V. M.; Peterson, I. R.; Kenn, R. M.; Shih, M. C.; Durbin, M.; Dutta, P. *J. Chem. Phys.* **1995**, *102*, 9412.

(13) Scalas, E.; Brezesinski, G.; Möhwald, H.; Kaganer, V. M.; Bouwman, W. G.; Kjaer, K. *Thin Solid Films* **1996**, *284/285*, 56.

(14) Tanaka, M.; Schneider, M. F.; Brezesinski, G. *Chem. Phys. Chem.* **2003**, *4*, 1316.

(15) Hamley, I. W.; Skov, Pedersen, J. *J. Appl. Crystallogr.* **1994**, *27*, 29.

(16) Skov, Pedersen, J.; Hamley, I. W. *J. Appl. Crystallogr.* **1994**, *27*, 36.

(17) Braslau, A.; Deutsch, M.; Pershan, P. S.; Weiss, A. H.; Als-Nielsen, J.; Bohr, J. *Phys. Rev. Lett.* **1985**, *54*, 114.

(18) Pershan, P. S. *Faraday Discuss. Chem. Soc.* **1990**, *89*, 231.

(19) Dluhy, R. A. *Appl. Spectrosc. Rev.* **2000**, *35*, 315.

(20) Yun, W. B.; Bloch, J. M. *J. Appl. Phys.* **1990**, *68*, 1421.

(21) Kitaigorodski, A. I. *Organic Chemical Crystalography*; Consultants Bureau: New York, 1961.

(22) Skoda, W.; Hoekstra, L. L., van Soest, T. C.; Bennema, P.; van den Tempel, M. *Colloid Polym. Sci.* **1967**, *219*, 149.

(23) Israelachvili, J. N. *Intermolecular and Surface Forces*; Academic Press: San Diego, CA, 1985.

(24) Maltseva, E.; Shapovalov, V. L.; Möhwald, H.; Brezesinski, G. *J. Phys. Chem. B* **2006**, *110*, 919.